Temperature Dependence of Helical Structures of Poly(phenylacetylene) Derivatives Bearing an Optically Active Substituent

Kazuhide Morino,[a] Katsuhiro Maeda,[a] Yoshio Okamoto,[b] Eiji Yashima,*[a] and Takahiro Sato*[c]

Abstract: The temperature dependence of the helical conformations for the homopolymers of phenylacetylene derivatives bearing an optically active substituent, such as the (*R*)-((1-phenylethyl)carbamoyl)oxy and (*R*)-((1-(1-naphthyl)ethyl)carbamoyl)oxy groups at the phenyl group, and their copolymers with achiral phenylacetylenes were investigated in solution using circular dichroism (CD) and absorption spectroscopies. The magnitude of the induced CD (ICD) of the optically active homopolymers increased with decreasing temperature and was accompanied by a blueshift in their absorption maxima. On the other hand, the copolymers with achiral phenylacetylenes exhibited interesting ICD changes with temperature, depending on the bulkiness of the achiral comonomers. The copolymers with a less bulky phenylacetylene had a very intense ICD at low temperatures, the ICD pattern was almost opposite to those of the chiral homopolymers, while the copolymers with the most bulky phenylacetylene bearing a *tert*-butyldiphenylsiloxy group at the *para* position showed an ICD change similar to that of the optically active homopolymers. However, the copolymers with the phenylacetylene bearing a *tert*-butyldimethylsiloxy group with intermediate bulkiness at the *para* position showed no ICD change with temperature. These results indicate that the prevailing helix-sense of the chiral-achiral random copolymers of the phenylacetylenes is determined by a delicate interaction between the chiral and achiral side chains. The thermodynamic stability parameters for the helical conformations of the homopolymers and copolymers of the phenylacetylenes were estimated from the temperature dependence of the ICDs.

Keywords: chirality · circular dichroism · helical structures · polymerization · poly(phenylacetylene)

Introduction

Optically active helical polymers with an excess single-screw sense have drawn much attention not only because of their interesting structures as observed in various biopolymers, but also as a result of their possible applications to novel functional chiral materials in various fields, such as analytical chemistry and materials science.[1] Two types of helical polymers have so far been prepared. These can be classified based on the nature of their helical conformation; one is a stable (or static) helical polymer and the other is a dynamic helical polymer. Poly(triphenylmethyl methacrylate) (PTrMA) is an example of the former and one-handed, helical PTrMA has been prepared by asymmetric polymerization with optically active initiators (or catalysts).[1a,g] It is noteworthy that such a helical PTrMA with perfect one-handedness provides excellent optical resolution of many racemates when it is used as a chiral stationary phase (CSP) in high performance liquid chromatography (HPLC).[2] The latter group of helical polymers is exemplified by polyisocyanates[3] and polysilanes.[1e,f] Polyisocyanates are composed of long, alternating sequences of right- and left-handed helices separated by the helix reversal points that move along the polymer backbone, so that helix inversion readily occurs in solution; this indicates that the barriers for the helix inversion are very low. Therefore, the optically active polyisocyanates with a predominantly one-handed screw sense can be prepared by introducing a tiny amount of chiral bias to the polymer; for instance, the copolymer of an achiral isocyanate with a small amount of chiral isocyanate exhibits as high an optical activity as that of the chiral homopolymer.[3]

---

[a] Prof. Dr. E. Yashima, K. Morino, Dr. K. Maeda
Department of Molecular Design and Engineering
Graduate School of Engineering
Nagoya University, Chikusa-ku, Nagoya 464-8603 (Japan)
Fax: (+81) 52-789-3185
E-mail: yashima@apchem.nagoya-u.ac.jp

[b] Prof. Dr. Y. Okamoto
Department of Applied Chemistry
Graduate School of Engineering
Nagoya University, Chikusa-ku, Nagoya 464-8603 (Japan)

[c] Dr. T. Sato
Department of Macromolecular Science
Osaka University, Machikaneyama-cho 1-1
Toyonaka, Osaka 560-0043 (Japan)
Fax: (+81) 6-6850-5457
E-mail: tsato@chem.sci.osaka-u.ac.jp

0947-6539/02/0822-5112 $ 20.00+.50/0

Polyacetylenes are typical π-conjugated polymers consisting of conjugated double bonds in the main chain and they have been studied for use as novel polymeric materials, such as conducting materials, nonlinear optical materials, and gas-permeable membranes.[4] Furthermore, a helical conformation with a predominant helix-sense has been proposed as a possible conformation for the polyacetylenes obtained by the polymerization of acetylenes bearing an optically active side group by transition-metal catalysts, because they exhibit a characteristic induced circular dichroism (ICD) in the absorption region, which is attributed to the conjugated double bonds in the main chain (UV/Vis region).[5]

We previously reported that *cis–transoidal* poly(phenylacetylene) derivatives bearing an optically active carbamoyloxy group at the *para* position have an intense ICD in the UV/Vis region,[6a] and exhibit a high chiral recognition ability as a CSP in HPLC for various racemates, such as Tröger's base and spiropyran derivatives.[6b,c] In this case, the one-handed helical conformation of the polyacetylene appears to play an important role in the chiral recognition, since a stereo-irregular polyacetylene bearing the same chiral unit shows poor chiral recognition.[6b] We have also found that optically inactive, *cis–transoidal* poly(phenylacetylene)s bearing various functional groups, for instance, a carboxy group, an amino group, and a boronic acid residue, form a dynamic, predominantly one-handed helix upon complexation with optically active compounds capable of interacting with the functional groups. The complexes exhibit a characteristic ICD in the UV/Vis region, which reflects the stereochemistry, including the absolute configurations, of the chiral compounds.[7] These polymers can be used as a novel chiral sensory system. Moreover, we found that the induced helical chirality on a stereoregular poly((4-carboxyphenyl)acetylene) with optically active amines can be memorized by replacing the chiral amines with achiral amines.[8] Similar helicity induction could be possible for aliphatic polyacetylenes.[9] Recently, a detailed conformational study on optically active helical poly(propiolic ester)s was reported by Nomura and co-workers.[10] They demonstrated that the helical conformation of poly(propiolic ester)s was dynamic, similar to those of the polyisocyanates and polysilanes. They then experimentally estimated the energy barrier for the helix–helix interconversion ($\Delta G^{\neq}$) and the free energy difference between the helical and the reversal states (ΔG_r) by means of the variable-temperature NMR measurements. The ΔG_r values for the poly(propiolic ester)s are about only half as large as those of the polyisocyanates; this indicates that the helix reversals occur very often in poly(propiolic ester)s relative to polyisocyanates.

In a previous study, we investigated the effect of the bulkiness of the substituents on the phenyl groups of the achiral comonomers on the formation of the helical conformations derived from copolymers with optically active bulky phenylacetylenes in solution and found that the optical activity (CD intensity and specific rotation) of the copolymers at room temperature increased with increasing bulkiness of the achiral comonomers.[6a] However, helical conformations are often strongly dependent on temperature, and the dependence can give us important information on the cooperativity of the helical conformations, which has not yet been studied for poly(phenylacetylene)s.[5–8] In the present study, we investigated the temperature dependence of the CD and absorption spectra for the homopolymers of optically active phenylacetylene derivatives (**1**, **2**, **3**, **7**, and **8**) and the copolymers of optically active monomers (**1**, **2**, and **3**) with achiral comonomers (**4**, **5**, and **6**). The data were analyzed in order to estimate the thermodynamic parameters characterizing the stability of the helical conformations of the poly(phenylacetylene)s (Scheme 1).

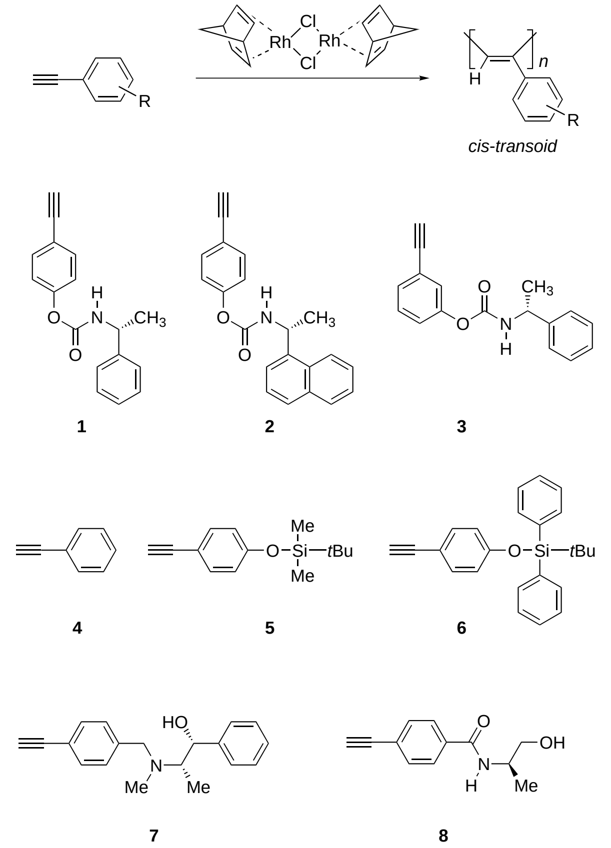

Scheme 1. Structures of poly(phenylacetylene)s, chiral (**1**–**3**, **7**, **8**), and achiral (**4**–**6**) phenylacetylene derivatives.

Results

Except for poly-**8** and poly($\mathbf{1}_4$-*co*-$\mathbf{4}_6$), we used optically active homopolymers and copolymers with achiral comonomers previously prepared by polymerization with $[Rh(nbd)Cl]_2$ (nbd: norbornadiene) according to Scheme 1.[6a, 11] The polymerization of a new chiral phenylacetylene derivative (**8**), bearing an amide group, was carried out with $[Rh(nbd)Cl]_2$ in tetrahydrofuran (THF) containing a small amount of triethylamine to give an orange, powdery polymer in moderate yield (60%). The ^{1}H NMR spectrum of poly-**8** in [D$_6$]dimethylsulfoxide (DMSO) had a sharp singlet centered at $\delta = 5.75$ due to the main chain protons, indicating that the polymer has a highly *cis-transoidal* stereoregular structure, based on the literature.[12] All other homopolymers and copolymers also have a highly *cis-transoid* structure, as previously reported.[6a, 11] The characteristics of the polymers employed in this

Table 1. Characteristics of homopolymers of phenylacetylenes bearing an optically active substituent and copolymers with achiral comonomers.

Run	Polymer[a]	M_1	M_2	$[M_1]$ in polymer (mol %)[b]	$M'_{w,S}$[c] ($\times 10^4$)	$N_{0,w}$[f] ($\times 10^3$)	UV/Vis ε/λ (nm)	$[\theta]_{2nd} \times 10^{-4}$ $/\lambda$ (nm)	Ref.
1	poly-**1**	**1**	–	100	200	6.8	2990/391	– 2.18/365	[6a]
2	poly($\mathbf{1}_1$-*co*-$\mathbf{4}_9$)	**1**	**4**	9.2	300	17	3200/388	0.14/374	[6a]
3	poly($\mathbf{1}_4$-*co*-$\mathbf{4}_6$)	**1**	**4**	44.1	21	1.2	3530/389	– 0.24/367	this work
4	poly($\mathbf{1}_1$-*co*-$\mathbf{5}_9$)	**1**	**5**	8.2	270	9.3	3140/407	– 0.58/373	[6a]
5	poly($\mathbf{1}_3$-*co*-$\mathbf{6}_7$)	**1**	**6**	29.7	730	26	3180/400	– 2.63/371	[6a]
6	poly-**2**	**2**	-	100	18	0.62	3060/395	– 1.48/369	[6a]
7	poly($\mathbf{2}_1$-*co*-$\mathbf{4}_9$)	**2**	**4**	13.7	130	7.2	3300/393	0.03/382	[6a]
8	poly($\mathbf{2}_1$-*co*-$\mathbf{5}_9$)	**2**	**5**	11.2	270	9.5	3290/408	– 0.82/371	[6a]
9	poly($\mathbf{2}_3$-*co*-$\mathbf{6}_7$)	**2**	**6**	28.2	660	23	3690/400	– 2.73/371	[6a]
10	poly-**3**	**3**	–	100	310	11	3880/405	– 0.01/357	[6a]
11	poly($\mathbf{3}_1$-*co*-$\mathbf{4}_9$)	**3**	**4**	13.5	130	7.3	3470/393	0.03/370	[6a]
12	poly($\mathbf{3}_1$-*co*-$\mathbf{5}_9$)	**3**	**5**	11.8	230	8.1	3500/413	–	[6a]
13	poly($\mathbf{3}_2$-*co*-$\mathbf{6}_8$)	**3**	**6**	20.4	630	22	3700/400	0.82/373	[6a]
14	poly-**7**	**7**	–	100	(10[d])		3510/409	0.33/372	[11]
15	poly-**8**	**8**	–	100	27[e]	1.5	2820/400	– 1.49/377	this work

[a] The subscript numbers represent the molar ratio of monomer units in copolymers. [b] Estimated by ^{1}H NMR. [c] Apparent weight-average molecular weight determined by SEC (polystyrene standard) with THF as the eluent. [d] Apparent number-average molecular weight determined by SEC (pullulan standard) with DMSO as the eluent. [e] Determined by SEC (poly(ethylene oxide) and poly(ethylene glycol) standard) with DMF containing LiCl (10 mM) as the eluent. [f] Weight-average degree of polymerization estimated from $M'_{w,S}$ (see text).

study, including molecular weight, content of the optically active monomer units, and the UV/Vis and CD data, are summarized in Table 1.

In order to investigate the ability of the chiral monomer units to control the overall main chain helical conformation (a helix-sense bias) of the corresponding homopolymers and copolymers with various achiral comonomers, we examined the temperature-dependent chiroptical behaviors of the homopolymers and copolymers. The temperature-dependent changes in the CD and absorption spectra of the homopolymer of **1**, which has an optically active (*R*)-((1-phenylethyl)carbamoyl)oxy group at the *para* position, and the copolymers with various achiral comonomers (**4**, **5**, and **6**) are shown in Figure 1 and the ICD intensities of the second Cotton are plotted versus temperature (Figure 2 A).

Poly-**1** showed an intense, split-type ICD in the UV/Vis region due to a predominantly one-handed helical conformation in THF at room temperature as already reported (Figure 1 A).[6a] The magnitude of the poly-**1** ICD increased monotonically with decreasing temperature and almost reached a plateau value at around – 60 °C with a slight blueshift in the λ_{max} of the second Cotton by 8 nm. The absorption spectra of poly-**1** exhibited a large blueshift; the absorbance over 400 nm significantly diminished and a peak at around 320 nm increased with decreasing temperature. These CD and absorption spectral changes indicated that the helical screw sense preference of poly-**1** increased with a decrease in temperature and poly-**1** may have a rather tight helical (or an off-planar) conformation at lower temperatures. The third Cotton intensity at 310 nm of poly-**1** also increased with decreasing temperature, as shown in Figure 1 A. Although not shown in Figure 2, the ratio of the CD to UV peak heights at this wavelength, which may be equated to the Kuhn dissymmetric ratio, had the same temperature dependence as

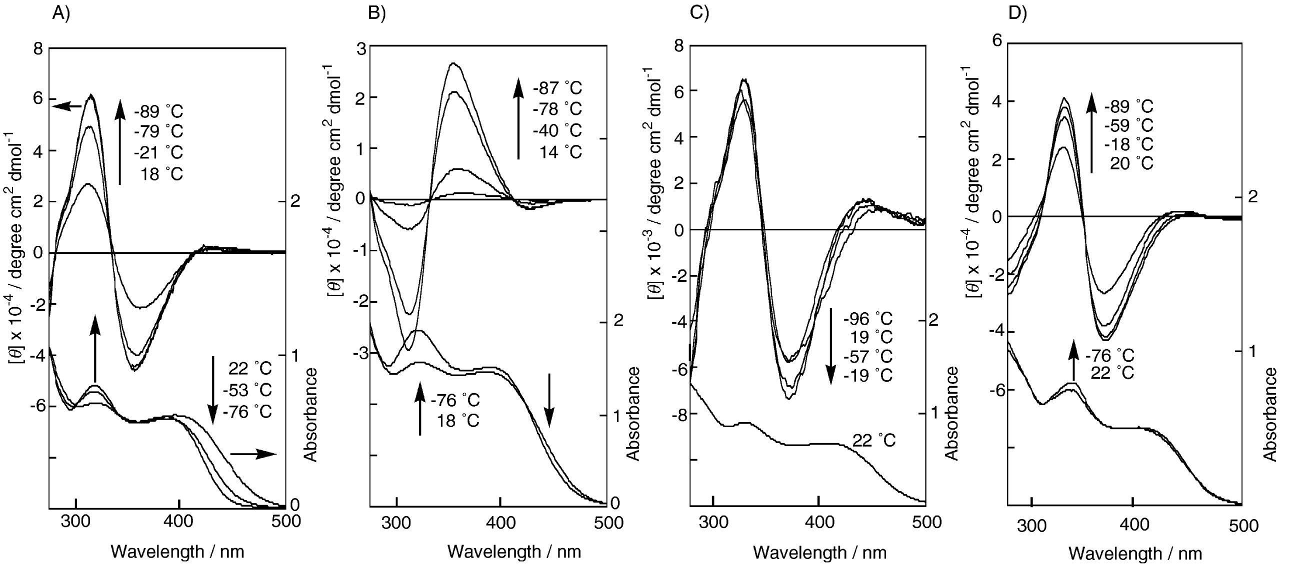

Figure 1. CD and absorption spectral changes of poly-**1** (A), poly($\mathbf{1}_1$-*co*-$\mathbf{4}_9$) (B), poly($\mathbf{1}_1$-*co*-$\mathbf{5}_9$) (C), and poly($\mathbf{1}_3$-*co*-$\mathbf{6}_7$) (D) in THF at various temperatures.

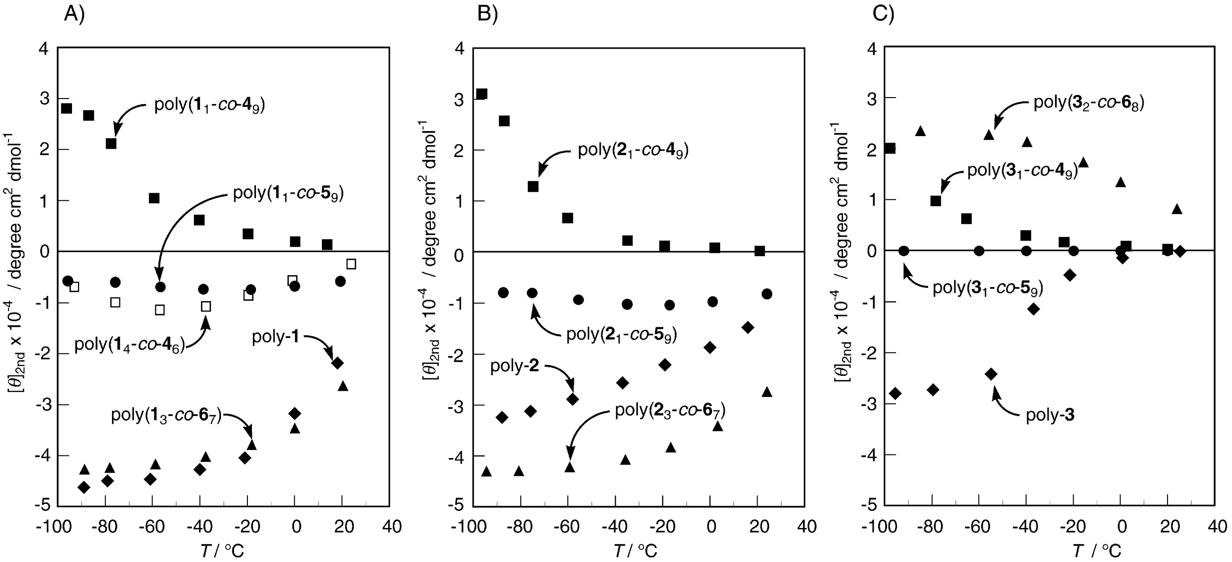

Figure 2. Temperature dependence of the molar ellipticity $[\theta]_{2nd}$ at the 2nd Cotton peak of the homopolymers (◆) and the copolymers of **1** (A), **2** (B), and **3** (C) with **4** (■, □), **5** (●), and **6** (▲) in THF.

that of the second Cotton peak. A very weak Cotton effect was observed at wavelengths longer than 400 nm. The reason for this effect is not clear at present.

The changes in the CD and absorption spectra of the copolymers of **1** with achiral comonomers (**4**, **5**, and **6**) with temperature were also investigated in THF, in order to explore the effect of the bulkiness of the substituents on the helical conformation of the poly(phenylacetylene)s. Previous results have shown that at room temperature the ICD intensities for the copolymers of **1** increased with an increase in the bulkiness of the substituents of the achiral comonomers.[6a] In fact, as shown in Figure 1 B–D, while the copolymer with the less bulky phenylacetylene, poly($\mathbf{1}_1$-*co*-$\mathbf{4}_9$), showed a very weak CD with opposite Cotton effects at 14 °C, the more bulky phenylacetylenes, poly($\mathbf{1}_1$-*co*-$\mathbf{5}_9$) and poly($\mathbf{1}_3$-*co*-$\mathbf{6}_7$), exhibit a stronger CD at room temperature. However, remarkable changes in the ICD intensity were observed for the copolymers of **1** with **4** at temperatures lower than −40 °C, and the ICD intensity at −87 °C was about 20 times greater than that at room temperature (Figures 1 B and 2 A). The sudden onset and rapid increase in the optical activity of the copolymer are indicative of cooperative interactions among the side chains, which appear to be important for understanding the nature of the conformation of the polyacetylenes (for detailed discussion, see below). Moreover, the ICD pattern of poly($\mathbf{1}_1$-*co*-$\mathbf{4}_9$) was almost a mirror image of that of poly-**1**, indicating that the predominant helix-sense of poly($\mathbf{1}_1$-*co*-$\mathbf{4}_9$) is opposite to that of poly-**1**. The absorption spectra of poly($\mathbf{1}_1$-*co*-$\mathbf{4}_9$) also showed a slight blueshift with decreasing temperature similar to poly-**1**. On the other hand, poly($\mathbf{1}_1$-*co*-$\mathbf{5}_9$), prepared by the copolymerization with the bulky comonomer **5**, was insensitive to any temperature change and the CD and absorption spectra hardly changed from 19 to −96 °C (Figure 1 C), while the copolymer of **1** with the bulkiest **6** (poly($\mathbf{1}_3$-*co*-$\mathbf{6}_7$)) exhibited an intense ICD, comparable to that of poly-**1**, in spite of the small content of the chiral monomer unit (29.7 %) at room temperature (Figure 1 D). Similar to poly-**1**, the magnitude of the ICD of poly($\mathbf{1}_3$-*co*-$\mathbf{6}_7$) monotonically increased as the temperature was lowered. However, in contrast with poly-**1** and poly($\mathbf{1}_1$-*co*-$\mathbf{4}_9$), the absorption spectra of poly($\mathbf{1}_3$-*co*-$\mathbf{6}_7$) did not show any appreciable change with temperature. This implies that the helix-sense excess of poly($\mathbf{1}_3$-*co*-$\mathbf{6}_7$) became greater at lower temperatures, but the helical structure, including the helical pitch, remained intact regardless of the temperature changes.

A similar temperature-dependent change in the Cotton effect was also observed for the homopolymer (poly-**2**) bearing an (*R*)-((1-(1-naphthyl)ethyl)carbamoyl)oxy group and a series of copolymers with achiral **4**, **5**, and **6** (Figure 2 B). Poly-**2** and the copolymer with **6** bearing the bulkiest substituent (poly($\mathbf{2}_3$-*co*-$\mathbf{6}_7$)) showed intense ICDs, even at about 20 °C, and the magnitude gradually increased with decreasing temperature. The ICD of the latter seems to be saturated at the same level as those of poly-**1** and (poly($\mathbf{1}_3$-*co*-$\mathbf{6}_7$)) at low temperatures. Poly($\mathbf{2}_1$-*co*-$\mathbf{4}_9$) showed almost no ICD in the range over 300 nm at about 20 °C, but below −60 °C, the ICD magnitude rapidly increased in a sigmoidal fashion with almost a mirror image in shape to those of poly-**2**, poly($\mathbf{2}_1$-*co*-$\mathbf{5}_9$), and poly($\mathbf{2}_3$-*co*-$\mathbf{6}_7$). Poly($\mathbf{2}_1$-*co*-$\mathbf{5}_9$) did not exhibit any apparent temperature dependence of the CD and absorption spectra. These results indicate that the predominant helix-sense is controlled by a delicate interaction between the chiral and achiral side chains.

To explore the effect of the position of an optically active substituent on the helical conformation of poly(phenylacetylene)s, the temperature dependence of the CD and absorption spectra of the homopolymer and copolymers of **3** bearing an (*R*)-((1-phenylethyl)carbamoyl)oxy group at the *meta* position was investigated (Figure 2 C). The homopolymer, poly-**3**, showed almost no ICD over 300 nm from approximately 20 to 0 °C, but as the temperature decreased further, an apparent ICD appeared and the ICD signal continued to increase in a sigmoidal fashion. These significant ICD changes were accompanied by a gradual blueshift in the absorption, as seen in poly-**1**. The Cotton effect signs of poly-**3** are the same as those of poly-**1** and poly-**2**, which indicates that the predominant helix-sense is the same for all of the homopolymers, and the substitution position of the optically active groups only slightly influences the helix-sense. Both of the copolymers with **4** and **5** showed negligibly weak ICD at about 20 °C, but a different temperature dependence was observed. Although a plot of the second Cotton intensity of poly($\mathbf{3}_1$-*co*-$\mathbf{4}_9$) versus temperature indicates a sigmoidal curvature with a positive sign, like the copolymers of **1** and **2** with achiral **4**, poly($\mathbf{3}_1$-*co*-$\mathbf{5}_9$) did not have any detectable ICD even at −92 °C. The copolymer of **3** with the most bulky **6** showed a relatively large ICD at about 20 °C, whose intensity increased with decreasing temperature, while its absorption spectra did not show a significant change. It is noteworthy that the Cotton effect signs of poly($\mathbf{3}_2$-*co*-$\mathbf{6}_8$) and poly($\mathbf{3}_1$-*co*-$\mathbf{4}_9$), being closely related to the helix-sense of the copolymers, were opposite to that of the homopolymer (poly-**3**). The copolymers with **4** and **6** possess a reversed helical structure compared with that of the poly-**3**. Based on these results, the introduction of an optically active substituent at the *para* position rather than the *meta* position may be effective in biasing the screw sense.

Comparison of these temperature-dependent changes in the ICDs as well as in the handedness of all the homopolymers, show a marked tendency in their behavior. Except for the copolymers with **5**, all of the homopolymers and copolymers showed an increase in the magnitude of the ICD with decreasing temperature. In particular, a dramatic increase of the Cotton effect in a sigmoidal fashion was observed for the copolymers with **4** and the homopolymer of **3** at lower temperatures. These temperature-dependent ICD changes occurred rapidly and were reversible. Similar and strong temperature-dependent changes in optical activity have been reported for typical dynamic helical polymers, such as polyisocyanates[3a–c, 13, 14] and polysilanes.[15] Therefore, these results strongly indicate that poly(phenylacetylene)s may also be classified into this category (dynamic helical polymer)s.

Moreover, the copolymers with **4** examined in this study showed an opposite Cotton effect sign as compared with those of the corresponding homopolymers (poly-**1**–poly-**3**) regardless of the position of the optically active substituents (*meta*- and *para* positions). The inversion of the Cotton effect indicates that there is a diastereomerically opposite chiral interaction between the side chains, which biases the reversed helix-sense. There could be another possibile explantation for such dramatic ICD changes with a reversed Cotton effect; it is the formation of aggregates, as previously reported for polyisocyanates, polysilanes, and other chiral π-conjugated polymers and oligomers.[3b, 16] However, we were able to exclude this possibility, since the CD and absorption spectral changes of poly($\mathbf{1}_1$-*co*-$\mathbf{4}_9$) were independent of the copolymer concentration (0.01–0.1 mg mL^{-1}). In order to obtain further information on the reason for the reversed Cotton effect of poly($\mathbf{1}_1$-*co*-$\mathbf{4}_9$), we prepared a poly(**1**-*co*-**4**) with 44 mol% of **1** units (poly($\mathbf{1}_4$-*co*-$\mathbf{4}_6$)) (run 3 in Table 1) and measured the temperature-dependent ICD changes (Figure 2 A). In contrast to poly($\mathbf{1}_1$-*co*-$\mathbf{4}_9$), poly($\mathbf{1}_4$-*co*-$\mathbf{4}_6$) exhibited a weak, but negative second Cotton effect; the sign is the same as poly-**1**, but opposite to that of poly($\mathbf{1}_1$-*co*-$\mathbf{4}_9$) and the magnitude of the ICD increases slightly with decreasing temperature (Figure 2 A). These results indicate that not only chiral monomers, but also the monomer sequences composed of chiral and achiral monomer units have a helix-sense bias to the overall polymer chain conformations. This composition-driven helix-sense inversion of copolymers consisting of chiral and achiral monomer units has already been observed for poly(phenyl isocyanate)s[14] and poly(dialkylsilane)s.[17] However, this is the first example of this phenomenon for polyacetylenes.

As can be seen in Figure 2, the copolymers with **5** (poly($\mathbf{1}_1$-*co*-$\mathbf{5}_9$), poly($\mathbf{2}_1$-*co*-$\mathbf{5}_9$), and poly($\mathbf{3}_1$-*co*-$\mathbf{5}_9$)) scarcely exhibited any ICD change with temperature. This seems to be associated with the moderate bulkiness of the substituent of **5** compared with those of **4** and **6**. The monomer sequence composed of achiral **5** and chiral **1** or **2** may not have a sufficiently strong bias of the helix-sense to move a helical conformation of the polymer backbone into a single screw sense.

As described above, the homopolymers of the optically active phenylacetylenes bearing a carbamoyloxy group (**1**–**3**) show a strong temperature dependence in their ICD intensities, which significantly increased with decreasing temperature. We then investigated if analogous optically active poly(phenylacetylene)s having a different chiral residue on the phenyl moiety would show similar ICD changes with temperature. Poly-**7** and poly-**8** were prepared and their temperature-dependent ICD changes were examined. As shown in Figure 3, both homopolymers also showed an increase in the ICD intensities when the temperature was lowered. These ICD changes were accompanied by a blueshift in the absorption similar to poly-**1**–poly-**3**. Based on these results, it can be concluded that optically active poly(phenylacetylene) derivatives have a dynamic helical conformation in nature.

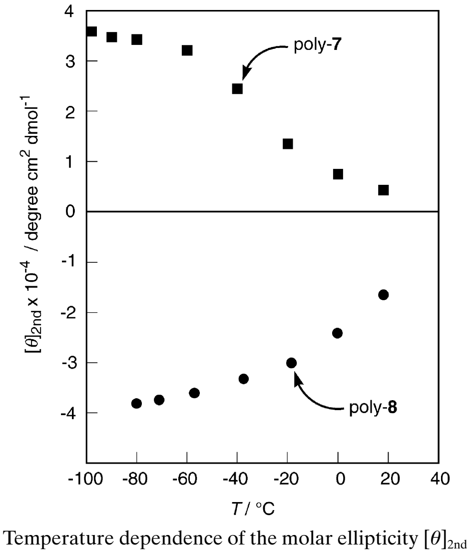

Figure 3. Temperature dependence of the molar ellipticity $[\theta]_{2nd}$ at the 2nd Cotton peak of poly-**7** (■) in THF and poly-**8** (●) in DMSO/MeOH 1:9 *v*/*v*.

Discussion

As shown in the previous section, homopolymers and copolymers of the phenylacetylene derivatives have a strong CD temperature dependence (except for the copolymers of **5**). This indicates that the helical conformation of each monomer unit in the polymers is determined by cooperative interactions with neighboring monomer units. The cooperative conformational transition of the helical polymers is usually treated in terms of the Ising model,[3a,b, 18] where each monomer unit in the helical polymer chains can take a right-handed (*P*) helical state, left-handed (*M*) helical state, or helix reversal state. In this section, we analyze the CD data presented in the previous section using this model to estimate the parameters determining the thermal stability of the helical conformation for the homo- and copolymers of the phenylacetylene derivatives.

According to Lifson and co-workers,[3a] the enantiomeric excess $2f_P - 1$ of the *P* state in helical homopolymers can be calculated as a function of the free energy difference $2\Delta G_{h,CC}$ between the *M* and *P* states, the excess free energy ΔG_r of the helix reversal state, the degree of polymerization N_0, and the absolute temperature *T*; $\Delta G_{h,CC}$ and ΔG_r are defined as the quantities per mole of the monomer unit, and the meaning of the subscript CC in $\Delta G_{h,CC}$ will be explained later. The molar ellipticity $[\theta]_{2nd}$ can then be calculated from $2f_P - 1$ multiplied by the maximum molar ellipticity $[\theta]_{max}$ of the intact P helix at $2f_P - 1 = 1$. In the following discussion, we tentatively assume that a positive $[\theta]_{max}$ corresponds to the P helix, although the relationship between the CD sign and the handedness of the helix has not yet been established for the poly(phenylacetylene) derivatives.

In a first approximation, we assume that $\Delta G_{h,CC}$ and ΔG_r are independent of *T*. Furthermore, for poly-**1** and poly-**2**, the chemical structures of the substituents are similar and also their CDs were measured in the same solvent, THF, so that we can expect that $[\theta]_{max}$ and ΔG_r for the two polymers are approximately the same. Under these conditions, we could almost uniquely determine the parameters of poly-**1** and poly-**2**. In the calculation of $2f_P - 1$, we used the weight-average degree of the polymerization listed in Table 1 as N_0, neglecting the effect of the polydispersity in N_0. The fitted results are shown by the solid curves for the two polymers in Figure 4, and the determined parameters are listed in Table 2. The substituent of poly-**8** is also not much different from those of poly-**1** and poly-**2**, and we can obtain a good fit for poly-**8** using similar values of $\Delta G_{h,CC}$, ΔG_r, and $[\theta]_{max}$; see Figure 4 and Table 2. (We did not analyze the CD data of poly-**7**, because we have no information about the weight-average molecular weight of this sample.)

We could not fit CD data of poly-**3** with a constant $\Delta G_{h,CC}$, but had to change it slightly with temperature.[13a] Although the fitting result (the curve in Figure 4) implies a temperature-driven helical screw-sense inversion at about 10 °C, which has already been observed in some polyisocyanates[14] and polysilylenes,[1e, 19] the experimental data do not clearly indicate it. The value of $[\theta]_{max}$ of this polymer is considerably smaller than those of the other four homopolymers. The *meta* substitution may change a local helical conformation, though the change is not reflected on the UV/Vis spectrum, which consists of multiple absorption bands.

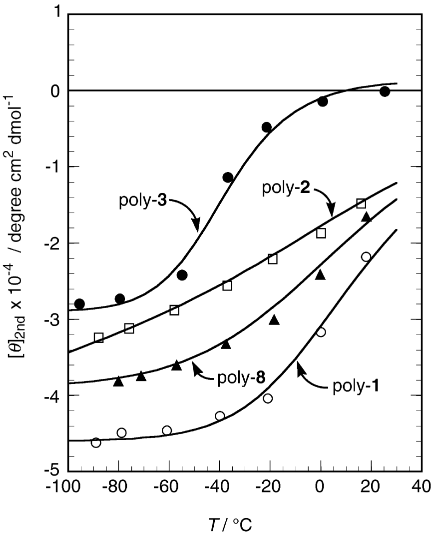

Figure 4. Comparison between experiment and theory of $[\theta]_{2nd}$ for the homopolymers of phenylacetylene derivatives. Solid curves represent theoretical values calculated by the Ising model theory with parameters listed in Table 2.

Table 2. Parameters determined by fitting CD data for poly(phenylacetylene) derivatives to the Ising model theory.

Run	Polymer	$[\theta]_{max}$[a]	$\Delta G_{h,CC}$[b]	$\Delta G_{h,CA}$[b]	ΔG_r[b]	Remarks
1	poly-**1**	4.6	– 2.4		15500	
2	poly(**1**$_1$-*co*-**4**$_9$)	4.6	– 2.4	7.1	10500	
3	poly(**1**$_4$-*co*-**4**$_6$)	4.6	– 2.4	0.21	15500	
5	poly(**1**$_3$-*co*-**6**$_7$)	4.2	– 2.4	– 7.5	15500	
6	poly-**2**	4.6	– 2.3		15500	
7	poly(**2**$_1$-*co*-**4**$_9$)	4.6	– 2.3	4.2	10500	
9	poly(**2**$_3$-*co*-**6**$_7$)	4.2	– 2.3	– 9.2	15500	
10	poly-**3**	2.9	– 0.60[c]		16700	at – 100 °C
		2.9	0.05[c]		16700	at 20 °C
11	poly(**3**$_1$-*co*-**4**$_9$)	4.4	same as poly-**3**	2.3	10500	
13	poly(**3**$_2$-*co*-**6**$_8$)	2.4	same as poly-**3**	5.4	15500	
15	poly-**8**	3.9	– 2.5		15500	

[a] In units of 10^4 degree cm^2 dmol^{-1}. [b] In units of J mol^{-1}. [c] $\Delta H_{h,CC}$ (the enthalpic component of $\Delta G_{h,CC}$) = – 1.54 J mol^{-1}; $\Delta S_{h,CC}$ (the entropic component of $\Delta G_{h,CC}$) = – 0.00544 J K^{-1} mol^{-1}.

The free energy difference, $\Delta G_{h,CC}$, is much smaller than the thermal energy for all the homopolymers listed in Table 2. This may come from the fact that the chiral center on the substituent of each of the homopolymers is remote from the backbone polyacetylene chain. On the other hand, all the ΔG_r values are much larger than the thermal energy, which indicates that helix reversal seldom occurs and monomer units tend to take a helical conformation of the same sense within the polymer chain.

Since the chiral centers of poly-**1**, -**2**, and -**3** are far from the polyacetylene backbone chain, chiral interactions should mainly be exerted between the side groups of the neighboring monomer units. Thus for the chiral – achiral random copolymers of **1**, **2**, and **3**, the free energy difference, $2\Delta G_h$, between the *P* and *M* helical states of each monomer unit may depend on the type of the interacting monomer unit.[20] We denote the ΔG_h value of the chiral unit interacting with the chiral and achiral units as $\Delta G_{\mathrm{h,CC}}$ and $\Delta G_{\mathrm{h,CA}}$, respectively; ΔG_{h} of the achiral unit interacting with the chiral unit may be identified with $\Delta G_{\mathrm{h,CA}}$, and $\Delta G_{\mathrm{h,AA}}$ should be zero from symmetry.

By generating many sequences of the chiral-achiral random copolymer with a given N_0 and mole fraction x of the chiral unit on a computer, we calculated the average conformational partition function to obtain f_{P} in the routine procedure.[18a] For such calculations, we have to choose the four parameters, $\Delta G_{\mathrm{h,CC}}$, $\Delta G_{\mathrm{h,CA}}$, ΔG_{r}, and $[\theta]_{\max}$ to fit the CD data of the copolymers. The first of these should be identical with that for the corresponding homopolymer, which has already been determined. The other three parameters may depend on the types of the chiral and achiral monomers; ΔG_{r} and $[\theta]_{\max}$ may also depend on x.

Since poly-**1** and poly-**2** have the same ΔG_{r} and $[\theta]_{\max}$ values (see Table 2), we may expect that these parameters for their copolymers with the same achiral monomer at the same x are also identical. Under this condition, we searched for the parameters leading to the best fit of the CD data of poly($\mathbf{1}_1$-*co*-$\mathbf{4}_9$), poly($\mathbf{2}_1$-*co*-$\mathbf{4}_9$), poly($\mathbf{1}_3$-*co*-$\mathbf{6}_7$), and poly($\mathbf{2}_3$-*co*-$\mathbf{6}_7$). The results are shown by the solid curves in Figure 5, and the parameters used are listed in Table 2. For the copolymers of **4**, $\Delta G_{\mathrm{h,CA}}$ and $\Delta G_{\mathrm{h,CC}}$ take the opposite sign, indicating that the chiral interaction between the chiral and achiral monomer units and between the chiral monomer units stabilizes the opposite helical state. The value of ΔG_{r} for the copolymers of **4** is smaller than those for the copolymers of **6**, while $[\theta]_{\max}$ for the latter is smaller than that for the former. The smaller ΔG_{r} may be due to the lower bulkiness of the substituent of **4**.

For poly($\mathbf{1}_4$-*co*-$\mathbf{4}_6$), we had to choose $\Delta G_{\mathrm{h,CA}}$ and ΔG_{r} values different from those of poly($\mathbf{1}_1$-*co*-$\mathbf{4}_9$) in order to obtain a good fit of the CD data, as shown by the solid curve in Figure 5A and Table 2. We can explain the increase in ΔG_{r} by increasing the content of the more bulky chiral monomer, but we have no suitable interpretation for the difference in $\Delta G_{\mathrm{h,CA}}$ between the same chiral and achiral pair.

For poly($\mathbf{3}_1$-*co*-$\mathbf{4}_9$), the chiral monomer content is so low that we may expect ΔG_{r} and $[\theta]_{\max}$ to be similar to those for poly($\mathbf{1}_1$-*co*-$\mathbf{4}_9$) and poly($\mathbf{2}_1$-*co*-$\mathbf{4}_9$). The fitting result for this copolymer is in accord with this expectation, as shown in Figure 5C and Table 2. On the other hand, we have to use a considerably smaller $[\theta]_{\max}$ for poly($\mathbf{3}_2$-*co*-$\mathbf{6}_8$) than those for poly($\mathbf{1}_3$-*co*-$\mathbf{6}_7$) and poly($\mathbf{2}_3$-*co*-$\mathbf{6}_7$) to obtain a good fit of the CD data. The reduction in $[\theta]_{\max}$ is, however, not reflected in the UV/Vis spectrum, as in the case of the poly-**3** homopolymer as mentioned above. We need more detailed analyses of the CD and UV/Vis spectra for the poly(phenylacetylene) derivatives.

As shown in Figure 2, $[\theta]_{\mathrm{2nd}}$ of all the copolymers containing **5** as the major component is essentially independent of temperature. Although the CD of poly($\mathbf{3}_1$-*co*-$\mathbf{5}_9$) may be explained by a compensation of $\Delta G_{\mathrm{h,CA}}$ and $\Delta G_{\mathrm{h,CC}}$, there is no parameter set which maintains $[\theta]_{\mathrm{2nd}}$ at a constant value except at zero and $\pm[\theta]_{\max}$ over a wide temperature range. One might regard these copolymers as stable (or static) helical polymers where the *P* and *M* helical states are not interconvertible, like the poly(triarylmethacrylate)s.[1a,g] However, the temperature dependent CD for the copolymers containing **6** with a more bulky substituent is in disagreement with this possibility. The constant CD values of poly($\mathbf{1}_1$-*co*-$\mathbf{5}_9$) and poly($\mathbf{2}_1$-*co*-$\mathbf{5}_9$) may be reproduced by the theory if $[\theta]_{\max}$ is as low as $1 \times 10^4\,\mathrm{degree\,cm^2\,dmol^{-1}}$ for these copolymers, but their UV-visible spectra are comparable to those for other poly(phenylacetylene)s.

Conclusion

A series of optically active poly(phenylacetylene)s consisting of chiral and achiral phenylacetylenes were prepared and their chiroptical properties as well as thermodynamic stability parameters for their helical conformations were investigated by low temperature CD measurements. It was found that the poly(phenylacetylene)s form a dynamic helical conformation like polyisocyanates, and the predominant helix-sense is governed by a delicate interaction between the chiral and

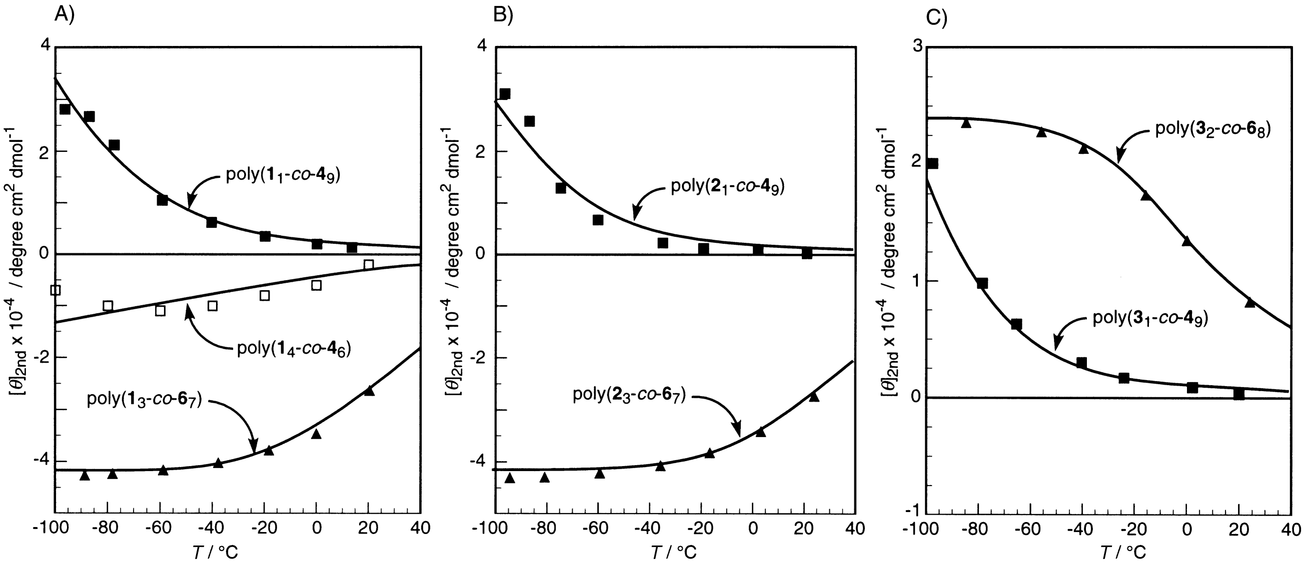

Figure 5. Comparison between experiment and theory of $[\theta]_{\mathrm{2nd}}$ for the copolymers of phenylacetylene derivatives. Solid curves represent theoretical values calculated by the Ising model theory with parameters listed in Table 2.

achiral side chains. These results should provide useful information for both understanding the mechanism of the helicity induction on optically inactive poly(phenylacetylene)s in the presence of chiral compounds[7] and the memory of the helical chirality,[8] as well as for designing novel helical poly(phenylacetylene)s.

Experimental Section

Instrumentation: Melting points were measured on a Büchi melting point apparatus and are uncorrected. Optical rotation was measured in a 5 cm quartz cell on a Jasco P-1030 polarimeter. NMR spectra were measured on a Varian VXR-500 (500 MHz for ^{1}H) or Varian Mercury 300 (300 MHz for ^{1}H) spectrometer in $CDCl_3$ or [D$_6$]DMSO using tetramethylsilane (for $CDCl_3$) or a solvent residual peak (for [D$_6$]DMSO) as the internal standard. Absorption spectra were measured with a Jasco V-570 spectrophotometer in a 0.1 cm quartz cell. The temperature was controlled in a homemade Dewar vessel equipped with a quartz window using methanol/ or acetonitrile/dry ice. CD spectra were measured on a Jasco J-725 spectropolarimeter with a liquid-nitrogen-controlled quartz cell (0.5 cm) in a cryostat. The concentration of polymers at low temperatures in THF was corrected by using the density of THF at the given temperature, but the concentration in DMSO/MeOH 1:9 was uncorrected. Size-exclusion chromatography (SEC) was performed with a Jasco PU-980 liquid chromatograph equipped with a UV/Vis (254 nm, Jasco UV-970) detector using Tosoh TSK-GEL α-3000 and α-5000 columns connected in series [eluent: *N*,*N*-dimethylformamide (DMF) containing LiCl (10 mM), standards: poly(ethylene oxide)s and poly(ethylene glycol)s].

Materials: THF was dried over sodium/benzophenone and distilled onto calcium hydride, followed by vacuum distillation onto $LiAlH_4$ under nitrogen. Triethylamine was dried over KOH pellets and distilled onto KOH under nitrogen. These solvents were distilled under high vacuum just before use. DMSO and DMF were dried over calcium hydride and distilled under reduced pressure. Methanol was dried over Mg and I_2 and distilled under nitrogen. 1-Hydroxybenzotriazole monohydrate (HOBt) was purchased from Wako (Osaka, Japan). *N*,*N*′-Dicyclohexylcarbodiimide (DCC) and *N*-methylmorpholine (NMM) were obtained from Kishida (Osaka, Japan). Bis[(norbornadiene)rhodium(I) chloride] ([Rh(nbd)Cl]$_2$) and (*R*)-(−)-2-amino-1-propanol were purchased from Aldrich. The synthesis of poly(phenylacetylene) derivatives, except for runs 3 and 15 in Table 1, have been previously reported.[6a, 11]

(*R*)-(−)-4-[((2-Hydroxy-1-methyl)ethyl)carbamoyl]phenylacetylene (8): HOBt (1.05 g, 6.86 mmol) and DCC (1.45 g, 7.03 mmol) at 0 °C were added to a solution of 4-ethynylbenzoic acid (1.00 g, 6.84 mmol), which had been prepared according to the previously reported method,[7d] in dry DMF (50 mL). After the reaction mixture was stirred at 0 °C for 1 h and at room temperature for 1 h under nitrogen, NMM (0.69 g, 6.8 mmol) and (*R*)-(−)-2-amino-1-propanol (0.65 g, 8.7 mmol) were added. The dispersion solution was stirred at room temperature for 20 h. After filtration, the solvent was removed under reduced pressure. The crude product was purified by silica gel chromatography with ethyl acetate as the eluent and then recrystallized from hexane/ethanol 8:3 to give a white crystalline solid (0.66 g, 47 %). M.p. 173.8–174.8 °C; $[\alpha]_D^{25} = -5°$ ($c = 0.5$ in MeOH); ^{1}H NMR (300 MHz, [D$_6$]DMSO): $\delta = 1.13$ (d, 3H; CH_3), 3.31–3.50 (m, 2H; CH_2), 3.95–4.06 (m, 1H; CH), 4.36 (s, 1H; ≡CH), 4.73 (t, 1H; OH), 7.56 (d, 2H; aromatic), 7.86 (d, 2H; aromatic), 8.18 (d, 1H; NH); ^{13}C NMR (75 MHz, [D$_6$]DMSO): $\delta = 17.1$ (CH_3), 47.4 (CH), 64.3 (CH_2), 82.6, 82.9 (HC≡C), 124.1, 127.4, 131.3, 134.7 (aromatic), 164.8 (C=O); IR (Nujol): $\tilde{\nu} = 3286$ (≡CH), 1634 (amide I), 1537 cm^{-1} (amide II); elemental analysis calcd (%) for $C_{12}H_{13}NO_2$ (203.2): C 70.94, H 6.40, N 6.90; found C 70.94, H 6.47, N 6.87.

Polymerization: Polymerization was carried out in a dry glass ampoule under a dry nitrogen atmosphere with [Rh(nbd)Cl]$_2$ as the catalyst. A typical polymerization procedure is described below. Monomer **8** (0.20 g, 0.98 mmol) was placed in a dry ampoule, which was then evacuated on a vacuum line flushed with dry nitrogen. After this evacuation-flush procedure was repeated three times, a three-way stopcock was attached to the ampoule, and THF and triethylamine were added with a syringe. A solution of a rhodium catalyst in THF at 30 °C was then added. The concentrations of the monomer and the rhodium catalyst were 0.2 and 0.002 M, respectively. The polymerization proceeded rapidly and an orange colored polymer precipitated within a few seconds. After 2 h, the resulting polymer was poured into a large amount of THF, collected by centrifugation, and dried in vacuo at 50 °C for 2 h (0.12 g, 60 %). ^{1}H NMR (300 MHz, [D$_6$]DMSO, 60 °C): $\delta = 1.11$ (d, 3H; CH_3), 3.41 (m, 2H; CH_2), 3.99 (m, 1H; CH), 4.64 (t, 1H; OH), 5.77 (s, 1H; =CH), 6.67 (singletlike, 2H; aromatic), 7.45 (singletlike, 2H; aromatic), 7.64 (singletlike, 1H; NH); IR (KBr): $\tilde{\nu} = 3300$ (N−H), 1637 (amide I), 1543 cm^{-1} (amide II). Poly(**1**$_4$-*co*-**4**$_6$) (run 3 in Table 1) was prepared in triethylamine according to the previously reported method.[6a]

Determination of the weight-average degree of polymerization ($N_{0,w}$): Apparent weight- and number-average molecular weights ($M'_{w,S}$ and $M'_{n,S}$) of homo- and copolymer samples of **1**, **2**, and **3** were determined by SEC with a calibration curve constructed by using polystyrene standard samples.[6a] On the other hand, $M'_{w,S}$ and $M'_{n,S}$ of newly prepared poly-**8** were estimated by SEC measurement calibrated with standard samples of poly(ethylene oxide)s and poly(ethylene glycol)s. The apparent molecular weight $M'_{w,S}$ may be related to the *true* weight-average degree of polymerization $N_{0,w}$ by the equation $[\eta]M_0N_{0,w} = [\eta]_S M'_{w,S}$, in which $[\eta]$ and M_0 are the intrinsic viscosity and monomer-unit molecular weight (the number-averaged one for copolymers) of the sample, respectively, and $[\eta]_S$ is the intrinsic viscosity of the standard sample with $M'_{w,S}$, which is reported in the literature.[21] For polymers of the same family with an identical backbone conformation, $[\eta]M_0$ is a unique function of $N_{0,w}$, irrespective of M_0. Therefore, if we know the function of $[\eta]M_0$ vs $N_{0,w}$ for the poly(phenylacetylene) family, we can estimate $N_{0,w}$ from $M'_{w,S}$ using the above equation. Recently, we obtained this function for poly((4-carboxyphenyl)acetylene) (PCPA) and also its complex with 1-(1-naphthyl)ethylamine (PCPA-Nap) in DMSO.[22] While the relation for PCPA in DMSO was demonstrated to be identical to that of poly(1-phenyl-1-propyne) (PPP) in toluene,[23] which is expected to have a similar backbone conformation to that of PCPA, $[\eta]M_0$ of the PCPA-Nap complex was larger than that of PCPA with the same $N_{0,w}$. This indicates that the complex becomes stiffer than PCPA because of the bulkiness of Nap binding to the side chain of PCPA. Since the bulkiness of side chains of all phenylacetylenes in the present study (except for **4**) is as large as that of the PCPA-Nap complex, we have used the $[\eta]M_0 - N_{0,w}$ relation for the complex to estimate $N_{0,w}$ of our polymer samples, except for the copolymers with **4**. For copolymer samples with **4**, the relation for PCPA or PPP was used. (Since there is no relation for the complex at high $N_{0,w}$, we have extrapolated $[\eta]M_0$ to higher $N_{0,w}$ using the theory of Yamakawa and co-workers[24] of $[\eta]$.)

Acknowledgements

We thank Professor K. Kobayashi (Nagoya University) for permission to use the cryostat apparatus for the CD measurements at low temperatures. This work was partially supported by Grant-in-Aid for Scientific Research from the Japan Society for the Promotion of Science and the Ministry of Education, Culture, Sports, Science, and Technology, Japan and the Inamori Foundation (K.M.). T.S. gratefully acknowledges CREST of JST for the financial support.

---

[1] a) Y. Okamoto, T. Nakano, *Chem. Rev.* **1994**, *94*, 349–372; b) K. Ute, K. Hirose, H. Kashimoto, O. Vogl, *J. Am. Chem. Soc.* **1991**, *113*, 6305–6306; c) R. J. M. Nolte, *Chem. Soc. Rev.* **1994**, *23*, 11–19; d) Y. Ito, T. Miyake, S. Hatano, R. Shima, T. Ohara, M. Suginome, *J. Am. Chem. Soc.* **1998**, *120*, 11880–11893; e) M. Fujiki, *J. Am. Chem. Soc.* **2000**, *122*, 3336–3343; f) M. Fujiki, *Macromol. Rapid Commun.* **2001**, *22*, 539–563; g) T. Nakano, Y. Okamoto, *Chem. Rev.* **2001**, *101*, 4013–4038 and references therein.

[2] a) Y. Okamoto, I. Okamoto, H. Yuki, S. Murata, R. Noyori, H. Takaya, *J. Am. Chem. Soc.* **1981**, *103*, 6971–6973; b) Y. Okamoto, K. Hatada, *J. Liq. Chromatogr.* **1986**, *9*, 369–384; c) Y. Okamoto, E. Yashima, *Prog. Polym. Sci.* **1990**, *15*, 263–298; d) E. Yashima, Y. Okamoto, *Bull. Chem. Soc. Jpn.* **1995**, *68*, 3289–3307; e) Y. Okamoto, E. Yashima, *Angew. Chem.* **1998**, *110*, 1072–1095; *Angew. Chem. Int. Ed.* **1998**, *37*, 1020–1043.

[3] a) S. Lifson, C. Andreola, N. C. Peterson, M. M. Green, *J. Am. Chem. Soc.* **1989**, *111*, 8850–8858; b) M. M. Green, N. C. Peterson, T. Sato, A. Teramoto, R. Cook, S. Lifson, *Science* **1995**, *268*, 1860–1866; c) K. Maeda, Y. Okamoto, *Macromolecules* **1998**, *31*, 1046–1052; d) S. K. Jha, K. S. Cheon, M. M. Green, J. V. Selinger, *J. Am. Chem. Soc.* **1999**, *121*, 1665–1673.

[4] a) H. Shirakawa, T. Masuda, K. Takeda in *The Chemistry of Triple-Bond Functional Groups* (Ed.: S. Patai), Wiley, New York, **1994**, Chapter 17; b) H. Shirakawa, *Angew. Chem.* **2001**, *113*, 2642–2648; *Angew. Chem. Int. Ed.* **2001**, *40*, 2574–2580; c) A. G. MacDiarmid, *Angew. Chem.* **2001**, *113*, 2649–2659; *Angew. Chem. Int. Ed.* **2001**, *40*, 2581–2590; d) A. J. Heeger, *Angew. Chem.* **2001**, *113*, 2660–2682; *Angew. Chem. Int. Ed.* **2001**, *40*, 2591–2611.

[5] a) F. Ciardelli, S. Lanzillo, O. Pieroni, *Macromolecules* **1974**, *2*, 174–179; b) J. S. Moore, C. B. Gorman, R. H. Grubbs, *J. Am. Chem. Soc.* **1991**, *113*, 1704–1712; c) M. Yamaguchi, K. Omata, M. Hirama, *Chem. Lett.* **1992**, 2261–2262; d) T. Aoki, M. Kokai, K. Shinohara, E. Oikawa, *Chem. Lett.* **1993**, 2009–2012; e) Y. Kishimoto, M. Itou, T. Miyatake, T. Ikariya, R. Noyori, *Macromolecules* **1995**, *28*, 6662–6666; f) L. Pu, *Acta Polym.* **1997**, *48*, 116–141.

[6] a) E. Yashima, S. Huang, T. Matsushima, Y. Okamoto, *Macromolecules* **1995**, *28*, 4184–4193; b) E. Yashima, S. Huang, Y. Okamoto, *J. Chem. Soc. Chem. Commun.* **1994**, 1811–1812; c) E. Yashima, T. Matsushima, T. Nimura, Y. Okamoto, *Korean Polym. J.* **1996**, *4*, 139–146.

[7] a) E. Yashima, T. Matsushima, Y. Okamoto, *J. Am. Chem. Soc.* **1995**, *117*, 11596–11597; b) E. Yashima, T. Nimura, T. Matsushima, Y. Okamoto, *J. Am. Chem. Soc.* **1996**, *118*, 9800–9801; c) E. Yashima, Y. Maeda, Y. Okamoto, *Chem. Lett.* **1996**, 955–956; d) E. Yashima, T. Matsushima, Y. Okamoto, *J. Am. Chem. Soc.* **1997**, *119*, 6345–6359; e) M. A. Saito, K. Maeda, H. Onouchi, E. Yashima, *Macromolecules* **2000**, *33*, 4616–4618; f) K. Maeda, S. Okada, E. Yashima, Y. Okamoto, *J. Polym. Sci. Part A*: *Polym. Chem.* **2001**, *39*, 3180–3189; g) H. Onouchi, K. Maeda, E. Yashima, *J. Am. Chem. Soc.* **2001**, *123*, 7441–7442.

[8] E. Yashima, K. Maeda, Y. Okamoto, *Nature* **1999**, *399*, 449–451.

[9] a) E. Yashima, H. Goto, Y. Okamoto, *Polym. J.* **1998**, *30*, 69–71; b) K. Maeda, H. Goto, E. Yashima, *Macromolecules* **2001**, *34*, 1160–1164.

[10] a) H. Nakako, R. Nomura, M. Tabata, T. Masuda, *Macromolecules* **1999**, *32*, 2861–2864; b) H. Nakako, Y. Mayahara, R. Nomura, M. Tabata, T. Masuda, *Macromolecules* **2000**, *33*, 3978–3982; c) R. Nomura, Y. Fukushima, H. Nakako, T. Masuda, *J. Am. Chem. Soc.* **2000**, *122*, 8830–8836.

[11] E. Yashima, Y. Maeda, Y. Okamoto, *Polym. J.* **1999**, *31*, 1033–1036.

[12] a) C. Simionescu, S. Dumitrescu, V. Percec, *J. Polym. Sci. Polym. Symp.* **1978**, *64*, 209–227; b) A. Furlani, C. V. Napoletano, M. V. Russo, W. J. Feast, *Polym. Bull.* **1986**, *16*, 311–317; c) M. Tabata, W. Yang, K. Yokota, *J. Polym. Sci. Part A*: *Polym. Chem.* **1994**, *32*, 1113–1120; d) Y. Kishimoto, P. Eckerle, T. Miyatake, M. Kainosho, A. Ono, T. Ikariya, R. Noyori, *J. Am. Chem. Soc.* **1999**, *121*, 12035–12044.

[13] a) H. Gu, Y. Nakamura, T. Sato, A. Teramoto, M. M. Green, C. Andreola, N. C. Peterson, S. Lifson, *Macromolecules* **1995**, *28*, 1016–1024; b) N. Okamoto, F. Mukaida, H. Gu, Y. Nakamura, T. Sato, A. Teramoto, M. M. Green, C. Andreola, N. C. Peterson, S. Lifson, *Macromolecules* **1996**, *29*, 2878–2884.

[14] K. Maeda, Y. Okamoto, *Macromolecules* **1999**, *32*, 974–980.

[15] K. Terao, Y. Terao, A. Teramoto, N. Nakamura, M. Fujiki, T. Sato, *Macromolecules* **2001**, *34*, 6519–6525.

[16] a) M. M. Green, C. A. Khatri, M. P. Reidy, K. Levon, *Macromolecules* **1993**, *26*, 4723–4725; b) S. Yue, G. C. Berry, M. M. Green, *Macromolecules* **1996**, *29*, 6175–6182; c) J-M. Guenet, H. S. Jeon, C. Khatri, S. K. Jha, N. P. Balsara, M. M. Green, A. Brulet, A. Thierry, *Macromolecules* **1997**, *30*, 4590–4596; d) H. Nakashima, M. Fujiki, J. R. Koe, M. Motonaga, *J. Am. Chem. Soc.* **2001**, *123*, 1963–1969; e) R. B. Prince, J. S. Moore, L. Brunsveld, E. W. Meijer, *Chem. Eur. J.* **2001**, *7*, 4150–4154.

[17] J. R. Koe, M. Fujiki, M. Motonaga, H. Nakashima, *Macromolecules* **2001**, *34*, 1082–1089.

[18] a) H. Gu, T. Sato, A. Teramoto, L. Varichon, M. M. Green, *Polym. J.* **1997**, *29*, 77–84; b) M. M. Green, J.-W. Park, T. Sato, A. Teramoto, S. Lifson, R. L. B. Selinger, J. V. Selinger, *Angew. Chem.* **1999**, *111*, 3329–3345; *Angew. Chem. Int. Ed.* **1999**, *38*, 3138–3154.

[19] M. Fujiki, J. R. Koe, M. Motonaga, H. Nakashima, K. Terao, A. Teramoto, *J. Am. Chem. Soc.* **2001**, *123*, 6253–6261.

[20] T. Sato, K. Terao, A. Teramoto, M. Fujiki, *Macromolecules* **2002**, *35*, 5355–5357.

[21] M. Kurata, Y. Tsunashima in *Polymer Handbook* (Eds.: J. Brandeup, E. H. Immergut), Wiley, New York, **1999**.

[22] Y. Ashida, T. Sato, K. Morino, K. Maeda, E. Yashima, unpublished results.

[23] T. Hirao, T. Sato, T. Norisuye, A. Teramoto, T. Masuda, T. Higashimura, *Polym. J.* **1991**, *23*, 925–932.

[24] T. Yoshizaki, I. Nitta, H. Yamakawa, *Macromolecules* **1988**, *21*, 165–171.

Received: April 15, 2002 [F4017]